Basic and Clinical
NEUROSCIENCE

March & April 2024, Vol 15, No. 2

Research Paper

Effect of Parenchymal Arachnoid on Brain Fluid Transport

Eric Hansen[1*], **Christopher Janson**[2], **Liudmila Romanova**[3], **Cornelius Lam**[4]

1. Department of Neurosurgery, Minneapolis Veterans Administration Health Care System, Minneapolis, United States.
2. Department of Internal Medicine and Neurology, Wright State University, Beavercreek, United States.
3. Department of Neurology and Rehabilitation, Medical School, University of Illinois Chicago, Chicago, United States.
4. Department of Neurosurgery, School of Medicine, University of Minnesota, Minneapolis, United States.

Use your device to scan and read the article online

Citation Hansen, E., Janson, Ch., Romanova, L., & Lam,C. (2024). Effect of Parenchymal Arachnoid on Brain Fluid Transport. *Basic and Clinical Neuroscience, 15*(2), 221-232. http://dx.doi.org/10.32598/bcn.2022.3089.1

http://dx.doi.org/10.32598/bcn.2022.3089.1

Article info:
Received: 30 Nov 2020
First Revision: 10 Nov 2021
Accepted: 27 Jun 2022
Available Online: 01 Mar 2024

Keywords:
Arachnoid, Brain parenchyma, Transport, Brain slice culture

ABSTRACT

Introduction: The pia-arachnoid is a critical component of cerebrospinal fluid removal. It covers and invaginates into the brain parenchyma, and physiologic failure results in hydrocephalus and cerebral edema. The purpose of this study was to characterize the role of arachnoid within brain parenchyma and determine if water flux and solute transport are affected by these intra-parenchymal cells.

Methods: An immortalized arachnoid rat cell line was used to seed 300-µm organotypic rat brain slices of 4-week-old rats. Fluid and tracer transport analyses were conducted following a 7-10 day intraparenchymal growth period. The development of an arachnoid brain slice model was characterized using diffusion chamber experiments to calculate permeability, diffusion coefficient, and flux.

Results: Labeled rat arachnoid cells readily penetrated organotypic cultures for up to 10 days. A significant reduction of dye and water flux across arachnoid-impregnated brain slices was observed after 3 hours in the diffusion chamber. Permeability decreased in whole brain slices containing arachnoid cells compared to slices without arachnoid cells. In comparison, a significant reduction of dextran across all slices occurred when molecular weights increased from 40 to 70 kDa.

Conclusion: Tracer and small molecule studies show that arachnoid cells' presence significantly impacts water's movement through brain parenchyma. Size differential experiments indicate that the permeability of solute changed substantially between 40 and 70 kDa, an essential marker of blood-CSF barrier definition. We have developed an arachnoid organotypic model that reveals their ability to alter permeability and transport.

*** Corresponding Author:**
Eric Hansen, PhD.
Address: *Department of Neurosurgery, Minneapolis Veterans Administration Health Care System, Minneapolis, United States.*
Tel: *+01 (612) 4672820*
E-mail: *hanse989@umn.edu*

Highlights

- Arachnoid cells proliferated within brain slice cultures for up to 10 days.
- A significant reduction of dye and water flux across slices cultured with arachnoid was observed compared to brain slice cultures without arachnoid.
- We have developed an organotypic model to study arachnoidal transport.

Plain Language Summary

In this study we use brain slice cultures to study dye, water and small molecule movement across the brain. We found that seeding brain slice cultures with arachnoid significantly diminished dye and water transport compared to brain slice cultures that did not have additional cells seeded. We also found small molecules greater that 70 kDA to have a reduction in the ability to pass through brain slices. Our study allows for further study of the arachnoid cells ability to alter transport in the brain.

1. Introduction

The pia-arachnoid (pial) membrane forms a physical barrier over the surface of the brain, which delimits blood and other substances and is an essential component of cerebrospinal fluid (CSF) flow (Hansen et al., 2017; Yasuda et al., 2013). The pia-arachnoid also invaginates deep into the brain, following blood vessels, and grows into the parenchyma during development (Kwee & Kwee, 2007). It has been hypothesized that the pia and the arachnoid have the same embryologic origin, derived from an ectodermal origin, the perimedullary mesenchyme (Adeeb et al., 2012). Forming thin sheaths that occupy the Virchow-Robin spaces, leptomeninges lines the small vessels responsible for the blood-brain barrier (BBB). While extra-parenchymal arachnoid granulation physiology has been explored in detail, questions about parenchymal and arachnoidal contribution to brain transport are unclear (Brinker et al., 2014). A better understanding of water flux in brain tissue is essential in many pathologic conditions, including trauma, tumor growth, and brain edema, and the pia-arachnoid, along with the ependyma, are the two critical components of the brain-CSF interface (Bacyinski et al., 2017; Brinker et al., 2014; Morris et al., 2016).

The mechanism of fluid and solute flux at the pia-arachnoid barrier between the subarachnoid space and CSF has remained an open question, and the extent of leptomeningeal barrier function at the interface between brain parenchyma and CSF is also poorly understood (Hladky & Barrand, 2014). In arachnoid tissue, tight junctions and other paracellular adhesions are the predominant components of the blood-CSF-barrier (BCB). Previous studies have shown that arachnoid cells form tight junctions within 5-7 days on 2-dimensional (2D) cultures (Holman et al., 2010; Lam et al., 2011). The tight junctions and extracellular matrix derived from arachnoid are key components in delimiting neuro-transport (Ichikawa-Tomikawa et al., 2011; Lam et al., 2012; Lam et al., 2013). Downstream effects of transport disruption include alterations in neighboring cell communications, function, and pathologic spread of disease.

We present a new model to determine arachnoids' effects on brain parenchyma using whole brain slices. Studying parenchymal arachnoid cells is challenging due to their proximal location to blood vessels. Arachnoid tissue can be difficult to isolate, culture, and track in situ, and determining their function within brain parenchyma can also be technically demanding. We have found no other studies that have attempted to examine the role of arachnoid in this location. While taking advantage of our robust cell lines, our initial whole brain slice approach mitigates the problem of observing cells out of their environment in isolation. We began by populating organotypic cultures with leptomeningeal cells to determine the viability of this model. Secondly, we examined whether transport through parenchyma is affected by the seeded arachnoid cells. With these cells interdigitating into the brain, we hypothesize that fluid and tracer transport are altered due to paracellular and transcellular effects. This model of deeply embedded arachnoid is currently the closest mimic of their function within brain parenchyma.

2. Materials and Methods

Brain slice preparation

Sprague Dawley rats (approximately 4 weeks old) were rapidly sacrificed (CO_2 and decapitation). A total of 18 rats were used. The brains were removed and glued with cyanoacrylate to the chuck of a water-cooled Leica VT1000A vibratome and trimmed with a razor. Under aseptic conditions, 300-µm thick whole-brain coronal sections were cut and collected in a sterile medium. The organotypic slices were placed on a 3.0-µm membrane insert (Millipore Sigma Corning Transwell Cat # CLS3492) in 6-well plates. Arachnoid cells grown separately in culture plates were labeled with CellTracker™ (Thermo Fisher Cat#CM-Dil C7000) and incubated at 37°C in a humidified atmosphere of 95% air and 5% CO_2 in culture media containing Eagle's MEM with 10% fetal bovine serum (FBS) (Millipore Sigma Cat#F2442), non-essential amino acids (Millipore Sigma), glutamine (Biowhittaker Inc., Walkersville, MD), streptomycin, and penicillin (Millipore Sigma-Aldrich Cat#P4333) at 10 µL/mL each. The medium was changed twice per week. Also, 4×10^4 arachnoid cells were trypsinized and centrifuged at 3000 rpm for 3 minutes; the resulting pellet was homogenized and seeded with media solution on top of each brain slice. The arachnoid cells labeled with CellTracker™ were designed to display fluorescence to daughter cells but not adjacent cells in the population. Brain slices (1 per well), with the addition of arachnoid cells, were cultured at 37°C and 5% CO_2 and incubated for up to 10 days with the medium changed twice per week. After 3, 7, and 10 days, membranes with brain slices were fixed in 10% formalin, monitored for arachnoid cell growth, and examined for apoptosis. The other brain slices were carefully placed and sealed in the PermeGear Side-Bi-Side© chambers for permeability measurements.

Arachnoid cell line

We used our previously developed immortalized arachnoid rat cell line harvested from 3-week-old Sprague-Dawley rats, which we established have barrier properties characteristic of the CSF-blood barrier (Janson et al., 2011; Lam et al., 2012). As previously described, the arachnoid cells were immortalized by pBABE puro-SV40 LT (Janson et al., 2011). Briefly, a clarified viral supernatant containing pBABE-puro-SV40 LT was applied to the arachnoid cell primary culture. Target cells were initially at a density of 4×10^4 cells/well of a six-well plate. Media was aspirated, and 3 mL virus-containing media was added per well. Polybrene (Cat # TR-1003 Millipore) was added to a final concentration of 4g/mL. After 12–18 h of incubation, virus-containing media was aspirated and replaced with fresh media to avoid polybrene toxicity and possible adverse effects from conditioned media. Cells transduced with pBABE-puro-SV40 LT were selected over 14 days with puromycin. To establish cell phenotype, cells were stained with cytokeratin 18 antibody (Prod # C-04, Abcam Inc.), vimentin (Prod #080552; Invitrogen), and desmoplakin I + II (Prod # ab106434, Abcam, Inc.). Double labeling of vimentin and desmoplakin was done to verify cell identification.

To verify the purity of the arachnoid cell isolations, cells were stained for potential contaminating cells: Muscle, fibroblasts, endothelial cells, glial cells, and neuronal cells. Myosin (Prod # MA1-35718; Fisher Sci.) was used to identify muscle cells; S100 (Prod # 13E2E2; BioGenex) and glial fibrillary acidic protein (GFAP, G-A-5; Cell Marque) were used to identify glial cells; CD31 (1A10; Cell Marque) was used to identify endothelial cells; smooth muscle actin (SMA asm-1; Novacastra) was used to identify fibroblasts. Neuronal nuclei (Prod # NeuN, MAB377; Millipore) were used to identify neuronal cells. Staining levels for the cells were compared to positive controls.

Arachnoid cell growth and apoptosis on brain slices

To determine if arachnoid cells cultured on brain slices survived and penetrated organotypic slices, 3 brain slices were fixed in 10% formalin at each time point (i.e. day 3, 7, and 10) and analyzed using a BioRad MRC-1024 single photon confocal microscope 1024 (BioRad Cell Science, UK). A total of 30 slices taken at 25-µm increments from brains were viewed at each time point. All slices examined confirmed arachnoid cell survivability within the organotypic brain slice. To determine the extent of apoptosis of arachnoid cells grown on brain slices compared to standard culture plates, control cells were seeded on two 12-mm Transwell membrane plates and grown to confluency (>2×10^5 cells per well) for up to 10 days. At each time point, the media was removed, cells were washed ×2 with cold PBS, and rinsed in binding buffer. FITC Annexin V and propidium iodide were added according to the manufacturer's instructions (FITC Annexin V apoptosis detection Kit, BD Pharmingen, San Diego, CA). Relative frequencies of apoptosis of cells grown on Transwells compared to brain slices were determined by measuring absorbance at the 455 nm wavelength.

Growth constant calculations

Randomly selected cultures (n=3) were selected to measure growth, whose curve is described by Equation 1.

1. $\ln (N_2/N_1)=k(t_2-t_1)$

, where N_1 equals the number of cells present in the population at time t_1 and N_2 equals the number of cells present at time t_2, and k is a specific growth constant for the population. During the exponential growth phase, k can be written as Equation 2:

2. $k=\ln_2/t_D$

, where t_D=generation or doubling time.

Diffusion and permeability measurements

Dye experiments

A PermeGear Side-Bi-Side chamber (PermeGear, Inc. 3.4 mL chamber, Hellertown, PA) was used to test the diffusion rate of brain slices implanted with arachnoid cells. Controls of brain slices grown with fibroblast (n=6) and brain slices alone (n=6) were used. The temperature was maintained at 37˚C, and a brain slice was placed on a 3.0-µm porous membrane. The membrane and brain (n=6 for each treatment) were carefully sealed between the chambers. At the start of the experiment, indigo carmine (Millipore Sigma Cat #73436, St Louis, MO) diluted 1:10 was added to the donor chamber. At 10-minute intervals, 20-µL samples were taken from the receiver chamber, and the dye concentration (as a percentage of the donor compartment) was determined using a Packard SpectraCount photometric microplate reader (Packard Instrument Co., Meriden, CT).

A quantitative analysis of indigo carmine diffusion across organotypic slices was conducted using Fick's law. Diffusion (D) was calculated using Equation 3:

3. $D=-\Phi/(c_1-c_2/x_1-x_0)$

, where (c_1-c_2/x_1-x_0) is the concentration gradient. The net flow is the number of moles that pass a certain plane per second (Φ). D is the diffusion constant that is defined as the amount of a substance (in Mol) that diffuses through an area (cm^2) at a concentration gradient of 1 (Mol/cm).

Water flux experiments

The diffusion chamber was fitted with a manometer to test the water flux of brain slices implanted with arachnoid cells under 4- and 8-cm pressure gradients. Applying a hydraulic pressure difference of 4 and 8 cm H_2O over a 2-h time allowed us to measure the volumetric flow rate (J_v) under differences in pressure (n=6 for each pressure). The displacement of water was tracked and converted to J_v according to Equation 4:

4. $J_v=(\Delta d/\Delta t)\times F$

, where $\Delta d/\Delta t$ is the displacement rate, and F is a tube calibration factor (fluid volume occupying a known length of tubing). Because each chamber contained the same medium (DMEM), there was no osmotic pressure difference across the cell layer. Flux was obtained by measuring the volume of water displaced in the donor compartment per cm^2/s.

Dextran experiments

For large molecule transport studies, FITC labeled dextran of sizes 10, 40, 70, and 150 kDa (Sigma-Aldrich Co., St. Louis, MO) were placed in the donor compartment of the diffusion chamber (n=6 for each size). Briefly, dextran was dissolved in warm HBSS (Hank's balanced salt solution, including $NaHCO_3$ at 0.33 g/L with HEPES buffer [0.01 M]), producing 2.5 mg/mL of test solutions. The initial dextran concentration was obtained by sampling the donor chamber at time 0. Samples of 100 µL were taken from the receiving chamber every 30 minutes for 6 hours to calculate permeability. Samples were placed on a 96-well plate, and 100 µL of 40 mg/mL NaOH aqueous solution was added to each sample. Fluorescence was measured via excitation and emission wavelengths of 485 and 530 nm, respectively. All signals were measured using a Packard SpectraCount© photometric microplate reader (Packard Instrument Co., Meriden, CT) with control plates subtracted out.

The apparent in vitro permeability coefficient (Papp) was determined using Equation 5:

5. $P_{app}=\frac{Flux}{C_t\times A}$

, where C_t is the donor compartment concentration at time 0, A is the surface area of the Transwell filter (1.1 cm^2), and flux is the slope of dye concentration over time.

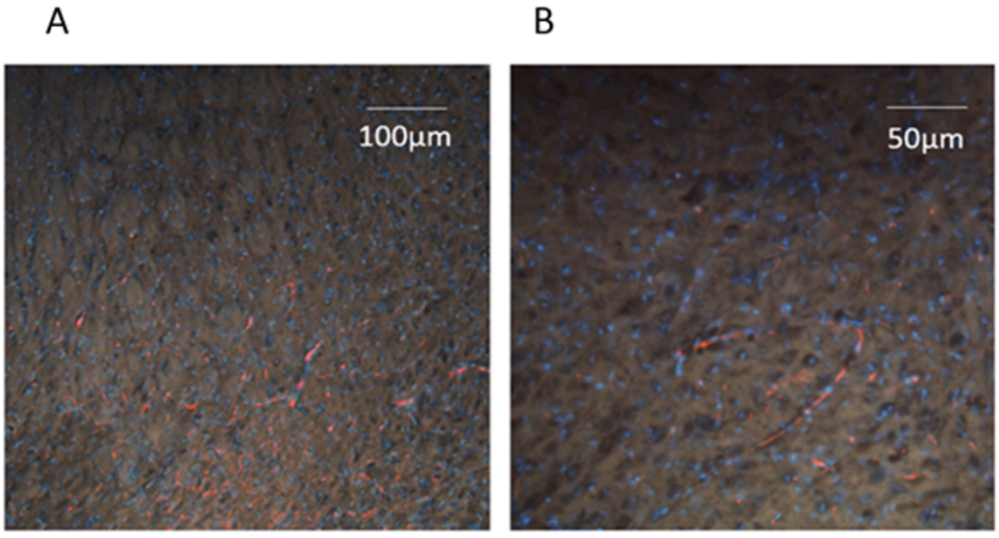

Figure 1. Brain slice cultured at 7 days with adding labelled arachnoid cells (red)

NEUROSCIENCE

Note: Nuclear staining is with DAPI (4′,6-diamidino-2-phenylindole). The image was taken at 100 µm depth using a BioRad MRC-1024 single photon confocal microscope 1024 merged with Brightfield (BioRad Cell Science, UK) (A taken at x10 magnification, B taken at x20 magnification).

Effective permeability (P) was determined using Equation 6:

$$6.\ \frac{1}{P}=\frac{1}{P_{app}}=\frac{1}{P_{m}}$$

, Where P_m is the dye's permeability across a membrane without an organotypic slice.

3. Results

Arachnoid cells labeled with CellTracker showed consistent and uniform growth into the brain slice (Figure 1). Initially, cells were observed to be scattered uniformly on the brain surface with some minor clustering but without monolayer formation. Arachnoid cells penetrated the brain slice within 2-4 days following seeding. No pattern of clusters or specific formations was observed within the brain slice. However, cells were regularly observed around blood vessels (Figure 2A). The cells exhibited a range of morphologies, from bipolar and tripolar spindles (Figure 2B) during the migration phase to a more robust polygonal shape as cells became established. Processes with lengths of greater than 100 µ were occasionally seen, and the orientation of the processes was similar to that seen in the native tissues (rat and human cultures) (Grzybowski et al., 2007; Rutka et al., 1986).

The growth phase occurred between day 2 and day 7. A growth constant of k=0.023 was used, corresponding to a doubling time of 30.4 hours (Figure 3A). No significant change in apoptosis occurred within the first 10 days of growth compared to arachnoid cells grown on culture plates (Figure 3B), indicating that apoptosis did not diminish total arachnoid cell growth during the acute phase and that cells mimicked 2D cultures. Figure 4 shows gradual increased arachnoid growth and a consistent pattern of minimal apoptosis throughout the experimental periods.

Brain slices grown with arachnoid cells had significantly less indigo carmine concentration in receiver compartments than brain slices grown with fibroblasts and brain slices alone in samples taken after 2 hours ($P<0.05$ for repeated measures ANOVA) (Figure 5). A curve was fitted to the data, and the diffusion coefficient for indigo carmine was calculated as $8.5\pm0.8 \times10^{-7}$ cm^2/s. Determining water transport is clinically important, given that edema is prevalent in many pathologic conditions. With a 4 cm water pressure gradient, a higher volume of water passed through brain slices with no arachnoid cells present after 3 hours compared to brain slices with arachnoid cells ($P<0.05$ for one-way ANOVA). An 8-cm water pressure gradient showed no significant difference in flux between brain slices with and without arachnoid cells after 2 hours ($P=0.29$ for one-way ANOVA) (Figure 6). Tight junctions were observed around arachnoid cell populations throughout the brain slice (Figure 7).

When molecules are too large to cross a membrane by diffusion, other methods exist to transport them into or out of the cell. The use of large dextran molecules can lead to information as to the role of inter-cellular trans-

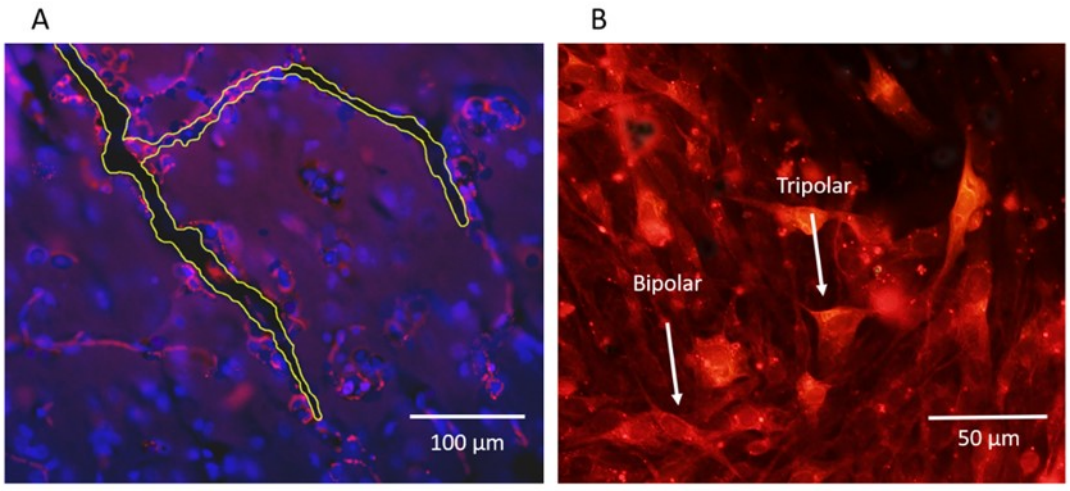

NEUROSCIENCE

Figure 2. Brain slice cultured at 7 days with adding labelled arachnoid cells (red) including nuclear staining DAPI (4',6-diamidino-2-phenylindole) (blue)

A) The yellow outline indicates blood vessels within the brain slice, with the arachnoid growing nearby, the image was taken at x40 magnification and 100 µm depth; B) Shows a brain slice cultured for 4 days, showing bipolar and tripolar morphology of arachnoid cells (red)

Note: The image was taken at x60 magnification and 50 µm depth using a BioRad MRC-1024 single photon confocal microscope 1024 (BioRad Cell Science, UK).

port channels. However, Figure 8 showed little difference in FITC labeled dextran permeability. There was no significant transport difference between brain slices with and without arachnoid cells. Nevertheless, significantly higher permeabilities were recorded with dextran 10 and 40 kDa compared to dextran 70 and 150 kDa ($P<0.05$ for one-way ANOVA), with an apparent size differential break between 40 and 70 kDa for both organotypic slice and organotypic slice with arachnoid cells.

4. Discussion

Arachnoid granulations and protrusions are typically within extra-parenchymal venous sinuses (Carpenter, 1991; Leach et al., 1996; Sakka et al., 2011). However, this study analyzed the role of arachnoid cells invading deep into the brain parenchyma. These arachnoid tissues have the same origins as the pia, and while the pia is densely adherent to the brain surface, they do not form

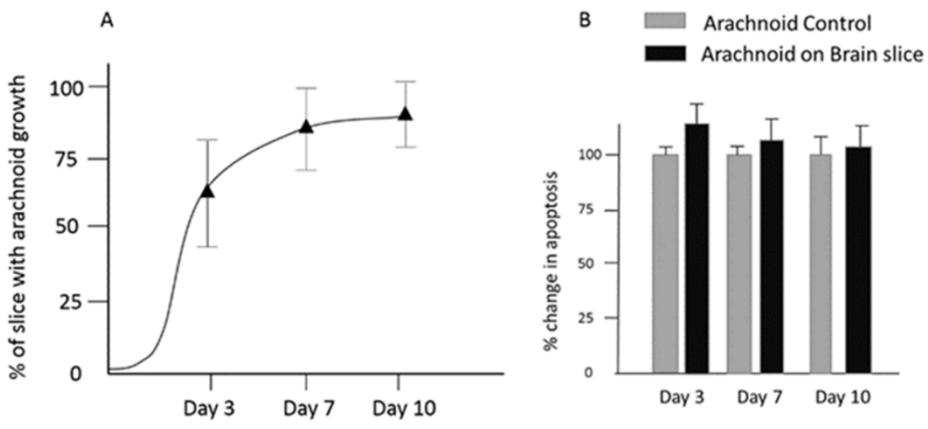

Figure 3. Growth of arachnoid cells on organotypic brain slices

NEUROSCIENCE

A) The arachnoid cells grew in brain slices, with cell populations eventually reaching a limiting size at approximately 10 days following seeding, B) Limited apoptosis in brain slices was observed over 10 days with no significant difference between organotypic slices and arachnoid cell controls (one-way ANOVA P=0.34)

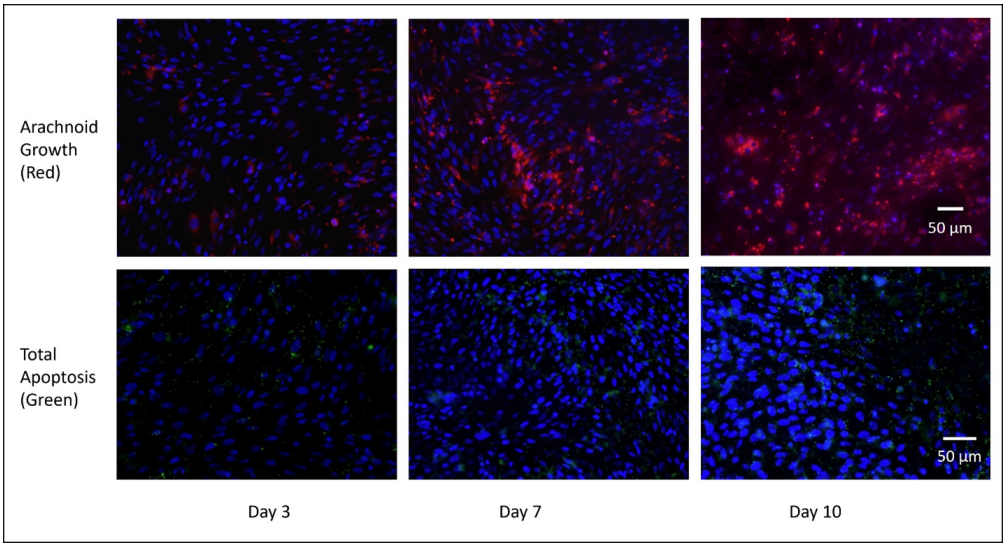

Figure 4. Arachnoid (red) across the top line showing increased growth within brain slices over 10 days NEUROSCIENCE

Note: Consistently low apoptosis (green) across the bottom row was recorded throughout the same growth period. The image was taken at 10x magnification at a 150 µm depth using a BioRad MRC-1024 single photon confocal microscope 1024 (BioRad Cell Science, UK).

barriers (Engelhardt et al., 2016). In contrast, arachnoid cells that penetrate the brain may be important in transport and barrier formation. As they follow Virchow Robin spaces, arachnoid line blood vessels with other endothelial cells form part of the blood-brain barrier to the brain parenchyma (Ek et al., 2006). Studying these cells in this location is exceedingly difficult. The isolation of arachnoid cells from this location would take them out of their natural environment, which is currently impossible. As the cells serve as a liaison between the endovascular space and the parenchyma, their role would require study close to native neural tissues such as astrocytes and neurons. We have used an organotypic culture model because it maintains the microarchitecture of the natural brain.

Organotypic brain slice culture models have proven useful in investigating cellular and molecular processes of the brain in in vitro studies (Drexler et al., 2010; Kim et al., 2013; Morin-Brureau et al., 2013), but these

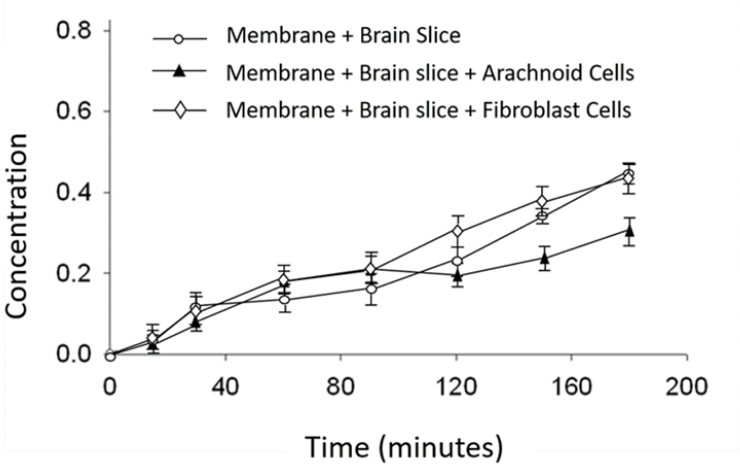

NEUROSCIENCE

Figure 5. Cells grown on transwell membranes allowed to reach confluency occurring at approximately 7 days in culture

Note: Membranes were placed in the diffusion chamber, and the concentration of indigo carmine dye in the receiver compartment was recorded over time. By 2.5 hours, the concentration of indigo carmine in brain slices grown with arachnoid was significantly less than in brain grown with fibroblast and brain slices alone. By hour 3, the concentration of indigo carmine in controls was almost double that of concentration in receiver compartments with brain slices.

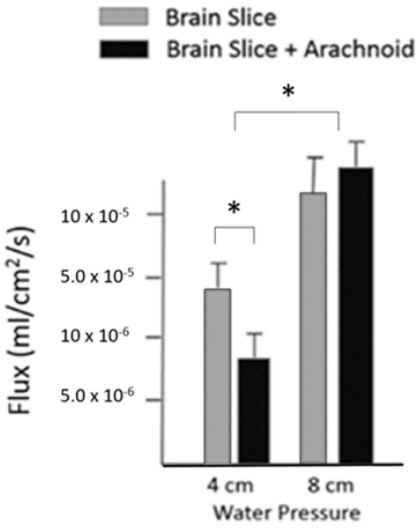

Figure 6. Cells grown on transwell membranes allowed to reach confluency

NEUROSCIENCE

Note: Chamber experiments under pressure conditions showed a significant increase in flux at 4 cm water pressure where brain slices did not contain arachnoid cells.

constructs have only been used to study CSF dynamics and barrier formation in a limited fashion (i.e. survival of cells, neurotoxicity assays, vascular damage, rate of drug delivery, protein regulation). Their advantage includes mimicking an environment impossible within in vitro monolayer systems (Czupalla et al., 2014). Other advantages include direct observation of cell-to-cell contacts in their normal positions and duplication of the microenvironment surrounding the relevant cells. Reproduction of physiologic chemical gradients is possible given the anatomic compartmentalization with defined flow vectors and pressure gradients found in pathologic conditions but with clear compartmentalization of tissue (Daneman & Prat, 2015; Morin-Brureau et al., 2013; Nag et al., 2011).

The survival of cells grown on brain slice cultures can vary greatly among tissues and over time (Humpel, 2015). We found the arachnoid cells grew readily into brain slices and reached a population limit around day 10. Most cells were located within 100 µm of the brain surface, with minimal apoptosis after 10 days. Arachnoid cells had normal appearing polygonal morphologies, consistent cell process numbers, and maintained their phenotype in the 3D organotypic environment. Though dense patterns or specific formations were not observed,

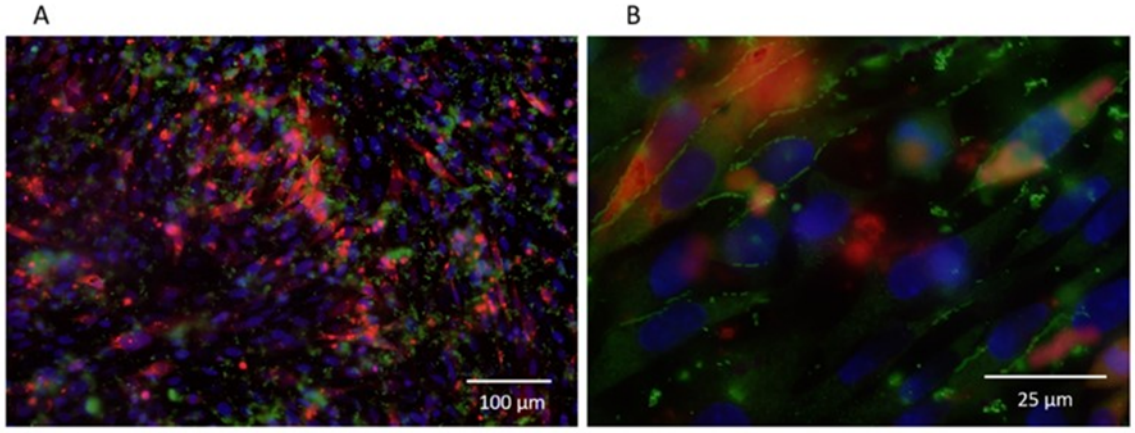

Figure 7. Brain slices cultured for 7 days to monitor tight junction formation

NEUROSCIENCE

A) Claudin-5 staining (green) and labeled arachnoid (red), taken at 100 µm depth at x10 magnification, B) X60 magnification using a BioRad MRC-1024 single photon confocal microscope 1024 (BioRad Cell Science, UK)

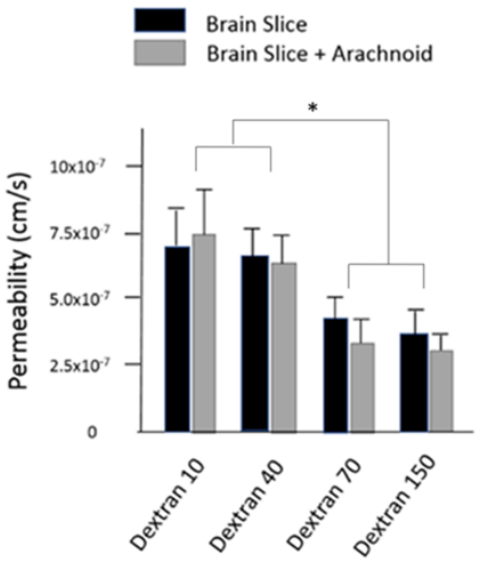

NEUROSCIENCE

Figure 8. Brain slices cultured for 7 days, the permeability of FITC labelled dextran (10, 40, 70 and 150 KDa) across brain slices with and without adding arachnoid cells

Note: Significantly higher permeabilities were recorded with dextran 10 and 40 kDa than with dextran 70 and 150 kDa ($P<0.05$ for one-way ANOVA).

arachnoid cells were regularly found around blood vessels, similar to what is found in vivo (Carpenter, 1991; Leach et al., 1996). As CSF is reabsorbed into venous sinus blood via arachnoid granulations, it is comprehensible that arachnoid cells gravitate towards these areas and may be supported by vasculature endothelial growth factors (VEGF). In vitro studies have shown that the VEGF family stimulates neuronal cell growth, migration, and sprouting (D'Amore, 2007). They are neuroprotectants in models of ischemic/hypoxic injury in the central nervous system (Góra-Kupilas & Jośko, 2005). Enhancement of VEGF in future organotypic studies may help determine the arachnoid response to different stimuli. In this study, the limited arachnoid saturation into deeper portions of the brain slice may be a consequence of competitive interactions with other neuroectodermal cells (Ozdil et al., 2020), apoptosis, or environmental factors like limited oxygen availability (Chopard et al., 1993; Ramírez et al., 2011) or gas exchange.

In the majority of organotypic models, the restriction of paracellular transport can be controlled by various mechanisms and components, including cell height, paracellular space tortuosity, tight junctions, gap junctions (Harhaj & Antonetti, 2004; Holman et al., 2010; Stoppini et al., 1991), and neuronal and glial-endothelial cell relationships (Duport et al., 1998; Tontsch & Bauer, 1991; Weller et al., 2018). In this study, the extracellular component of the arachnoid CSF sink appeared important in the transport of fluid and small molecular weight molecules. Brain slices cultured with arachnoid cells permitted less dye to pass through tissue than organotypic slices without arachnoid cells, presumably by forming tight junctions with neighboring glial cells, neurons, and astrocytes. Previous in vivo analysis of human granulations and cells grown on 2D membranes and 3D scaffolds have shown tight junction formation by electron microscopy and immunostaining within 7 days of culturing (Grzybowski et al., 2007; Holman et al., 2010). From our tracer, small molecule, and radioactive water studies (Lam et al., 2011, 2012), it is clear that the presence of arachnoid cells also impacted the movement of water through brain parenchyma. The effect was most marked after 2 hours. Our model was constrained to low pressures as the impact of the arachnoid was not visible once the pressure of 8 cm had been reached. Cytologic barriers, such as gap junctions and tight junctions, may be overwhelmed by bulk flow when pressures exceed this mark. As a consequence, the diffusion of molecules should occur in a compact parenchyma, as it happens in vivo (Brinker et al., 2014; Carpenter, 1991). The variable pressure gradients used in our system could be useful for assessing how brain tissue permeability changes through time and among different environmental factors. Determining water transport at different pressures is clinically important, given that edema is prevalent in many pathologic conditions.

Although organotypic cultures are powerful tools for studying paracellular transport, it is important to be aware of their limitations. One drawback to organotypic experimentation includes the risk of hypoxia, which does not mimic the brain's natural environment. While several parameters influence oxygen diffusion, such as slice thickness, matrix stiffness, and metabolic activity (Naipal et al., 2016; Wang & Andreasson, 2010), our organotypic brain slice tissue model represents a solid model for short- to medium-term barrier and transport assays. However, mass transport did not appear to be altered by the presence of arachnoid cells. Directly comparing this with monolayers is difficult because of the underlying presumptions of mannitol permeability, and trans-epithelial electrical resistance studies used in the Transwell model cannot be used as a surrogate for barrier formation in brain slices (Vernon et al., 2011). We show that the molecular weight profiles match what is expected for barrier formation with a cutoff of around 40 kDa, indicating the parenchyma volumetrically still maintains barrier properties throughout. Our data support the concept of the brain as a porous media and have shown that intra-parenchymal-arachnoid can affect its transport physiology. Like BBB and choroid plexus cells, arachnoid cells can express drug transport proteins and likely contribute to the blood-CSF drug permeation barrier (Yasuda et al., 2013). We have demonstrated that arachnoid cells appear to preferentially affect bulk flow over mass transport of material in a barrier-defined regime. Future work using our organotypic model should include further development of mass transport assays.

5. Conclusion

In summary, we provide evidence that arachnoid cells grown in organotypic slices possess similar characteristics found in vivo. We have demonstrated that diffusion is altered in the presence of arachnoid and that changes in pressure can modify arachnoid behavior at the brain-leptomeningeal interface. This model has applications to model several important diseases involved in fluid and solute transport at the brain-CSF interface, including hydrocephalus, subarachnoid hemorrhage, traumatic brain injury, brain tumors, stroke, and Alzheimer disease.

Ethical Considerations

Compliance with ethical guidelines

All applicable international, national, and or institutional guidelines for the care and use of animals were followed.

Funding

The work was supported by the VA Merit Review (Grant No.: #1I01BX001657-01).

Authors' contributions

Conceptualization and writing: All Authors; Supervision: Cornelius Lam; Experiments: Eric Hansen and Liudmila Đomanova.

Conflict of interest

The authors declared no conflict of interest

References

Adeeb, N., Mortazavi, M. M., Tubbs, R. S., & Cohen-Gadol, A. A. (2012). The cranial dura mater: A review of its history, embryology, and anatomy. *Child's Nervous System, 28*(6), 827–837. [DOI:10.1007/s00381-012-1744-6]

Bacyinski, A., Xu, M., Wang, W., & Hu, J. (2017). The paravascular pathway for brain waste clearance: Current understanding, significance and controversy. *Frontiers in Neuroanatomy, 11*, 101. [DOI:10.3389/fnana.2017.00101]

Brinker, T., Stopa, E., Morrison, J., & Klinge, P. (2014). A new look at cerebrospinal fluid circulation. *Fluids and Barriers of the CNS, 11*, 10. [DOI:10.1186/2045-8118-11-10]

Carpenter, M. B. (1985). *Core text of neuroanatomy*. Baltimore: Williams & Wilkins. [Link]

Chopard, R. P., Brancalhão, R. C., Miranda-Neto, M. H., & Biazotto, W. (1993). Arachnoid granulation affected by subarachnoid hemorrhage. *Arquivos de Neuro-Psiquiatria, 51*(4), 452–456. [DOI:10.1590/s0004-282x1993000400005]

Czupalla, C. J., Liebner, S., & Devraj, K. (2014). In vitro models of the blood-brain barrier. *Methods in Molecular Biology, 1135*, 415–437. [DOI:10.1007/978-1-4939-0320-7_34]

D'Amore P. A. (2007). Vascular endothelial cell growth factor-A: Not just for endothelial cells anymore. *The American Journal of Pathology, 171*(1), 14–18. [DOI:10.2353/ajpath.2007.070385]

Daneman, R., & Prat, A. (2015). The blood-brain barrier. *Cold Spring Harbor Perspectives in Biology, 7*(1), a020412. [DOI:10.1101/cshperspect.a020412]

Drexler, B., Hentschke, H., Antkowiak, B., & Grasshoff, C. (2010). Organotypic cultures as tools for testing neuroactive drugs-Link between in-vitro and in-vivo experiments. *Current Medicinal Chemistry, 17*(36), 4538–4550. [DOI:10.2174/092986710794183042]

Duport, S., Robert, F., Muller, D., Grau, G., Parisi, L., & Stoppini, L. (1998). An in vitro blood-brain barrier model: Cocultures between endothelial cells and organotypic brain slice cultures. *Proceedings of the National Academy of Sciences of the United States of America, 95*(4), 1840-1845. [DOI:10.1073/pnas.95.4.1840]

Ek, C. J., Dziegielewska, K. M., Stolp, H., & Saunders, N. R. (2006). Functional effectiveness of the blood-brain barrier to small water-soluble molecules in developing and adult opossum (monodelphis domestica). *The Journal of Comparative Neurology, 496*(1), 13–26. [DOI:10.1002/cne.20885]

Engelhardt, B., Carare, R. O., Bechmann, I., Flügel, A., Laman, J. D., & Weller, R. O. (2016). Vascular, glial, and lymphatic immune gateways of the central nervous system. *Acta Neuropathologica, 132*(3), 317–338. [DOI:10.1007/s00401-016-1606-5]

Góra-Kupilas, K., & Jośko, J. (2005). The neuroprotective function of vascular endothelial growth factor (VEGF). *Folia Neuropathologica, 43*(1), 31-39. [Link]

Grzybowski, D. M., Herderick, E. E., Kapoor, K. G., Holman, D. W., & Katz, S. E. (2007). Human arachnoid granulations Part I: A technique for quantifying area and distribution on the superior surface of the cerebral cortex. *Cerebrospinal Fluid Research, 4*, 6.[DOI:10.1186/1743-8454-4-S1-S6]

Hansen, E. A., Romanova, L., Janson, C., & Lam, C. H. (2017). The effects of blood and blood products on the arachnoid cell. *Experimental Brain Research, 235*(6), 1749–1758. [DOI:10.1007/s00221-017-4927-2]

Harhaj, N. S., & Antonetti, D. A. (2004). Regulation of tight junctions and loss of barrier function in pathophysiology. *The International Journal of Biochemistry & Cell Biology, 36*(7), 1206–1237. [DOI:10.1016/j.biocel.2003.08.007]

Hladky, S. B., & Barrand, M. A. (2014). Mechanisms of fluid movement into, through and out of the brain: Evaluation of the evidence. *Fluids and Barriers of the CNS, 11*(1), 26.[DOI:10.1186/2045-8118-11-26]

Holman, D. W., Kurtcuoglu, V., & Grzybowski, D. M. (2010). Cerebrospinal fluid dynamics in the human cranial subarachnoid space: An overlooked mediator of cerebral disease. II. In vitro arachnoid outflow model. *Journal of the Royal Society, Interface, 7*(49), 1205–1218. [DOI:10.1098/rsif.2010.0032]

Humpel C. (2015). Organotypic brain slice cultures: A review. *Neuroscience, 305*, 86–98. [DOI:10.1016/j.neuroscience.2015.07.086]

Ichikawa-Tomikawa, N., Sugimoto, K., Satohisa, S., Nishiura, K., & Chiba, H. (2011). Possible involvement of tight junctions, extracellular matrix and nuclear receptors in epithelial differentiation. *Journal of Biomedicine & Biotechnology, 2011*, 253048. [DOI:10.1155/2011/253048]

Janson, C., Romanova, L., Hansen, E., Hubel, A., & Lam, C. (2011). Immortalization and functional characterization of rat arachnoid cell lines. *Neuroscience, 177*, 23–34. [DOI:10.1016/j.neuroscience.2010.12.035]

Kim, H., Kim, E., Park, M., Lee, E., & Namkoong, K. (2013). Organotypic hippocampal slice culture from the adult mouse brain: A versatile tool for translational neuropsychopharmacology. *Progress in Neuro-Psychopharmacology & Biological Psychiatry, 41*, 36–43. [DOI:10.1016/j.pnpbp.2012.11.004]

Kwee, R. M., & Kwee, T. C. (2007). Virchow-robin spaces at MR imaging. *Radiographics, 27*(4), 1071–1086.[DOI:10.1148/rg.274065722]

Lam, C. H., Hansen, E. A., Hall, W. A., & Hubel, A. (2013). Application of transport phenomena analysis technique to cerebrospinal fluid. *Journal of Neurosurgical Sciences, 57*(4), 317–326.

Lam, C. H., Hansen, E. A., & Hubel, A. (2011). Arachnoid cells on culture plates and collagen scaffolds: Phenotype and transport properties. *Tissue Engineering. Part A, 17*(13-14), 1759–1766. [DOI:10.1089/ten.TEA.2010.0459]

Lam, C. H., Hansen, E. A., Janson, C., Bryan, A., & Hubel, A. (2012). The characterization of arachnoid cell transport II: Paracellular transport and blood-cerebrospinal fluid barrier formation. *Neuroscience, 222*, 228–238. [DOI:10.1016/j.neuroscience.2012.06.065]

Leach, J. L., Jones, B. V., Tomsick, T. A., Stewart, C. A., & Balko, M. G. (1996). Normal appearance of arachnoid granulations on contrast-enhanced CT and MR of the brain: Differentiation from dural sinus disease. AJNR. *American Journal of Neuroradiology, 17*(8), 1523-1532. [Link]

Morin-Brureau, M., De Bock, F., & Lerner-Natoli, M. (2013). Organotypic brain slices: A model to study the neurovascular unit micro-environment in epilepsies. *Fluids and Barriers of the CNS, 10*(1), 11. [DOI:10.1186/2045-8118-10-11]

Morris, A. W., Sharp, M. M., Albargothy, N. J., Fernandes, R., Hawkes, C. A., & Verma, A., et al. (2016). Vascular basement membranes as pathways for the passage of fluid into and out of the brain. *Acta Neuropathologica, 131*(5), 725–736. [DOI:10.1007/s00401-016-1555-z]

Nag, S., Kapadia, A., & Stewart, D. J. (2011). Review: Molecular pathogenesis of blood-brain barrier breakdown in acute brain injury. *Neuropathology and Applied Neurobiology, 37*(1), 3–23. [DOI:10.1111/j.1365-2990.2010.01138.x]

Naipal, K. A., Verkaik, N. S., Sánchez, H., van Deurzen, C. H., den Bakker, M. A., & Hoeijmakers, J. H., et al. (2016). Tumor slice culture system to assess drug response of primary breast cancer. *BMC Cancer, 16*, 78. [DOI:10.1186/s12885-016-2119-2]

Ozdil, B., Güler, G., Acikgoz, E., Kocaturk, D. C., & Aktug, H. (2020). The effect of extracellular matrix on the differentiation of mouse embryonic stem cells. *Journal of Cellular Biochemistry, 121*(1), 269–283. [DOI:10.1002/jcb.29159]

Ramírez, M. Á., Pericuesta, E., Yáñez-Mó, M., Palasz, A., & Gutiérrez-Adán, A. (2011). Effect of long-term culture of mouse embryonic stem cells under low oxygen concentration as well as on glycosaminoglycan hyaluronan on cell proliferation and differentiation. *Cell Proliferation, 44*(1), 75–85. [DOI:10.1111/j.1365-2184.2010.00732.x]

Rutka, J. T., Giblin, J., Dougherty, D. V., McCulloch, J. R., DeArmond, S. J., & Rosenblum, M. L. (1986). An ultrastructural and immunocytochemical analysis of leptomeningeal and meningioma cultures. *Journal of Neuropathology and Experimental Neurology, 45*(3), 285–303. [DOI:10.1097/00005072-198605000-00012]

Sakka, L., Coll, G., & Chazal, J. (2011). Anatomy and physiology of cerebrospinal fluid. *European Annals of Otorhinolaryngology, Head and Neck Diseases, 128*(6), 309–316. [DOI:10.1016/j.anorl.2011.03.002]

Stoppini, L., Buchs, P. A., & Muller, D. (1991). A simple method for organotypic cultures of nervous tissue. *Journal of Neuroscience Methods, 37*(2), 173–182. [DOI:10.1016/0165-0270(91)90128-m]

Tontsch, U., & Bauer, H. C. (1991). Glial cells and neurons induce blood-brain barrier related enzymes in cultured cerebral endothelial cells. *Brain Research, 539*(2), 247–253. [DOI:10.1016/0006-8993(91)91628-e]

Vernon, H., Clark, K., & Bressler, J. P. (2011). In vitro models to study the blood brain barrier. *Methods in Molecular Biology, 758*, 153–168. [DOI:10.1007/978-1-61779-170-3_10]

Wang, Q., & Andreasson, K. (2010). The organotypic hippocampal slice culture model for examining neuronal injury. *Journal of Visualized Experiments, 44*, 2106. [DOI:10.3791/2106]

Weller, R. O., Sharp, M. M., Christodoulides, M., Carare, R. O., & Møllgård, K. (2018). The meninges as barriers and facilitators for the movement of fluid, cells and pathogens related to the rodent and human CNS. *Acta Neuropathologica, 135*(3), 363–385. [DOI:10.1007/s00401-018-1809-z]

Yasuda, K., Cline, C., Vogel, P., Onciu, M., Fatima, S., & Sorrentino, B. P., et al. (2013). Drug transporters on arachnoid barrier cells contribute to the blood-cerebrospinal fluid barrier. *Drug Metabolism and Disposition, 41*(4), 923–931. [DOI:10.1124/dmd.112.050344]